

1 The ATLAS Trigger System - Ready for Run-2

Moritz Backes*

On behalf of the ATLAS Collaboration

CERN, Switzerland

E-mail: Moritz.Backes@cern.ch

The ATLAS trigger system successfully collected collision data during the first run of the LHC between 2009-2013 at a centre-of-mass energy between 900 GeV and 8 TeV. The trigger system consists of a hardware based Level-1 and a software based high-level trigger that reduces the event rate from the design bunch-crossing rate of 40 MHz to an average recording rate of a few hundred Hz. With the increased centre-of-mass energy of 13 TeV and the higher instantaneous luminosity expected during the Run-2 data-taking campaign the rates of Run-1 trigger selections would rise by approximately a factor of 5.

In these proceedings we briefly review the ATLAS trigger system upgrades that were implemented during the shutdown, allowing us to cope with the increased trigger rates while maintaining or even improving our efficiency to select relevant physics processes. This includes changes to the Level-1 calorimeter and muon trigger system, the introduction of a new Level-1 topological trigger subsystem and the merging of the previously two-level high-level trigger system into a single event filter farm. We show the performance improvements in the high-level trigger algorithms used to identify leptons, hadrons and global event quantities like missing transverse energy. Finally, we present the commissioning status of the trigger system and its initial performance in the 2015 run.

*XXVII International Symposium on Lepton Photon Interactions at High Energies
17-22 August 2015
Ljubljana, Slovenia*

*Speaker.



1. Introduction

The successful operation of the ATLAS trigger system [1] in the Run-1 data-taking campaign of the Large Hadron Collider (LHC) [2] at centre-of-mass energies between 900 GeV and 8 TeV laid the foundation for the extremely comprehensive and diverse Run-1 ATLAS physics program. With the increase in the centre-of-mass energy from 8 to 13 TeV, the expected rise of the peak luminosity from approximately $8 \times 10^{33} \text{cm}^{-2} \text{s}^{-1}$ to $1.5 \times 10^{34} \text{cm}^{-2} \text{s}^{-1}$ and the higher levels of pile-up interactions¹, the rates of the Run-1 trigger selections would rise by approximately a factor of 5 during the Run-2 data-taking campaign.

To deal with the increased trigger rates, while efficiently selecting the physics processes of interest, the ATLAS trigger system has undergone significant upgrades during the LHC shutdown period. In these proceedings the new features of the ATLAS trigger system are reviewed and first performance results from the commissioning of the upgraded system in the early phase of Run-2 are discussed.

2. ATLAS Trigger system upgrades for Run-2

A schematic overview of the Run-2 ATLAS trigger and data acquisition system is shown in Fig. 1. The trigger system consists of a hardware based first level trigger (L1) and a software based high-level trigger (HLT). The L1 trigger is implemented in custom electronics and determines Regions-of-Interest (RoIs) in the detector based on coarse calorimeter and muon detector information. The L1 trigger allows to reduce the event rate from the LHC bunch crossing rate (approximately 30 MHz expected for Run-2) to 100 kHz and forms a decision within $2.5 \mu\text{s}$. The regions of interest are then passed to the HLT which runs sophisticated reconstruction algorithms using full granularity detector information in either the RoI or the entire event to form a decision within an average processing time of 0.2 s. The output rate of the HLT is approximately 1 kHz on average.

As shown in Fig. 1 the L1 trigger consists of several sub-systems: The L1 calorimeter trigger, the L1 Muon trigger, and the L1 central trigger components.

The L1 calorimeter sub-system processes signals from the electromagnetic and hadronic calorimeter detectors and provides trigger signal inputs to the central trigger processor (CTP). An important new feature of the L1 calorimeter trigger in Run-2 is the use of new Multi-Chip Modules (nMCM) which are based on the field-programmable gate array (FPGA) technology while in Run-1 the corresponding modules were using application-specific integrated circuits (ASICs). The nMCMs enable the use of auto-correlation filters for improved energy resolution and a more flexible processing of the calorimeter signals with dynamic pedestal correction based on the global cell occupancy and timed with respect to the position of colliding bunches inside the proton bunch trains. These new features result in a significant reduction of the missing transverse² energy trig-

¹In Run-2 the average number of collisions per proton-proton bunch crossing is expected to reach approximately 40-45 compared to values of 25-30 in Run-1.

²ATLAS uses a right-handed coordinate system with its origin at the nominal interaction point (IP) in the centre of the detector and the z -axis along the beam pipe. The x -axis points from the IP to the centre of the LHC ring, and the y -axis points upward. Cylindrical coordinates (r, ϕ) are used in the transverse plane, ϕ being the azimuthal angle around the beam pipe. The pseudorapidity is defined in terms of the polar angle θ as $\eta = -\ln \tan(\theta/2)$.

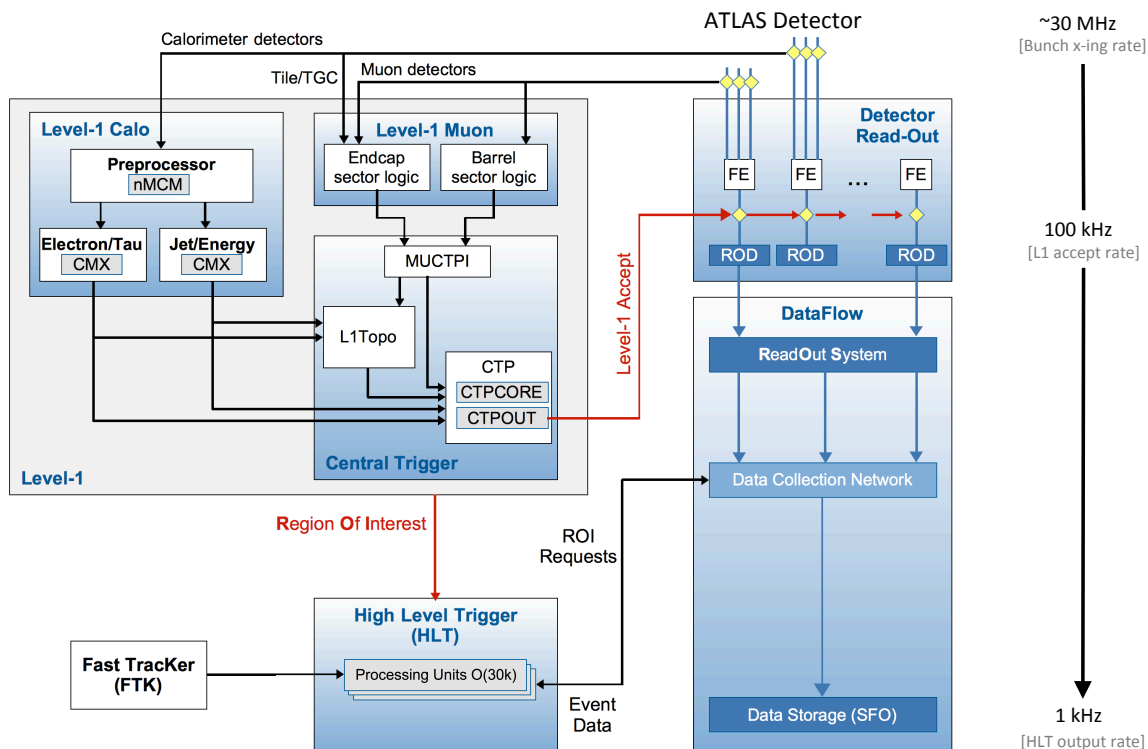


Figure 1: Schematic layout of the Run-2 ATLAS trigger and data acquisition system.

37 ger rates at L1 which were a major limitation in Run-1. In addition, the number of definable L1
 38 calorimeter trigger thresholds, such as for example electromagnetic, tau, jet, or missing transverse
 39 energy thresholds, was doubled with respect to Run-1 and provides added flexibility for the trigger
 40 selections.

41 In the L1 muon system, information from the inner end-cap muon chambers, which are in
 42 front of the end-cap toroid magnets, and from the extended barrel region of the Tile calorimeter are
 43 used in timing coincidences with the L1 muon system information already in place from Run-1.
 44 These new coincidences are expected to significantly decrease the the L1 muon trigger rates in
 45 the forward region ($1.0 < |\eta| < 1.9$) which are dominated by low- p_T out-of-time charged particles
 46 (e.g. protons) generated in the toroid magnet and the detector shielding. In addition, new trigger
 47 chambers in the feet of the detector barrel region are expected to bring a gain of approximately 4 %
 48 in acceptance for L1 muons at $|\eta| < 1.05$.

49 For Run-2 a conceptually new L1 topological sub-system (L1Topo) [3] is being put into place
 50 which performs topological selections based on L1 physics objects at the LHC bunch crossing rate.
 51 The L1Topo algorithms are implemented in FPGAs and form a decision within a latency of 200 ns.
 52 Examples of possible topological selections are angular and invariant mass requirements, or global
 53 event quantities such as the sum of the transverse momenta of all L1 jet objects. Topological trig-
 54 gers are crucial for the Run-2 physics program as they allow the energy and momentum thresholds
 55 for multi-object final states to be kept low while significantly decreasing the trigger rates.

56 The information of all L1 sub-systems is combined in the CTP which forms the final L1 trigger
 57 decision. The CTP has undergone a major upgrade for Run-2 and is now able to accommodate 512

58 L1 trigger thresholds (twice as many as in Run-1). In addition the CTP can now handle trigger
59 rates of up to 100 kHz which is a significant improvement over the 70 kHz limit in Run-1.

60 The HLT has also undergone significant upgrades for Run-2. The most important structural
61 change is the unification of the previously two-level system (Level-2 and Event Filter) into a single
62 event processing farm which reduces the overall complexity of the system and allows for dynamic
63 resource sharing between algorithms that were previously divided by being specific to one of the
64 two HLT trigger levels.

65 In this way an efficient coupling of the HLT selection steps is achieved which reduces the
66 duplication of CPU usage and network transfer of detector data. In addition, there has been a major
67 redesign of the Run-1 trigger reconstruction algorithms to be closer to the offline reconstruction
68 algorithms. The advantages of this approach are a large reduction in the duplication of online
69 and offline software, an easier commissioning and calibration of the triggers along with offline
70 selections and an increased physics acceptance after analysis selections. Furthermore, the HLT
71 algorithms now have the capability to use real-time pile-up information to correct for effects of
72 multiple interactions per bunch crossing.

73 3. Commissioning and performance of the ATLAS Trigger system in early Run-2

74 The upgraded ATLAS trigger system is currently being commissioned. In this section, the
75 performance of the main physics triggers in the initial phase of Run-2 with 50 ns proton bunch
76 spacing is discussed.

77 Fig. 2 (top left) shows the combined L1 and HLT efficiency of a single electron trigger (denoted
78 HLT_e24_lhmedium_loose_L1EM18VH) as a function of the electron candidate's transverse en-
79 ergy reconstructed 'offline' in the final data processing. The efficiency is measured with respect to
80 these fully reconstructed electrons that are required to pass likelihood-based "lhmedium" identifi-
81 cation. The trigger requires an electron candidate with $E_T > 24$ GeV satisfying the likelihood-based
82 "lhmedium" identification criteria as well as a loose track isolation requirement. The HLT trigger
83 is seeded by a level-1 trigger (L1_EM18VH) that applies an E_T dependent veto against energy
84 deposited in the hadronic calorimeter behind the electron candidate's electromagnetic cluster. The
85 efficiencies are measured with a tag-and-probe method using $Z \rightarrow ee$ decays with no background
86 subtraction applied. They are compared to expectation from $Z \rightarrow ee$ simulation. The error bars
87 show the statistical uncertainties only. Fig. 2 (top right) shows output rates of various single elec-
88 tron triggers as a function of the instantaneous luminosity in early Run-2. It can be seen that the
89 rates for electron triggers with likelihood-based identification criteria ("lhmedium" and "lhtight")
90 are lower than those corresponding to triggers with cut-based identification selections ("medium"
91 and "tight"). More details can be found in [reference PoS LP15 proceedings: "The Upgrade and
92 Performance of the ATLAS Electron and Photon Triggers towards Run II" by Joseph Reichert].

93 Fig. 2 (middle left) shows the efficiency of a L1 single muon trigger (denoted L1_MU15) and
94 the OR of the HLT_mu20_loose_L1MU15 and HLT_mu50 high-level triggers as a function of the
95 transverse momentum of offline muon candidates in the endcap detector region. The L1_MU15
96 trigger requires that a candidate passed the 15 GeV threshold requirement of the L1 muon trigger
97 system. The efficiency is computed relative to the offline muon candidates which are reconstructed
98 using standard ATLAS software and are required to pass "medium" quality requirement. The

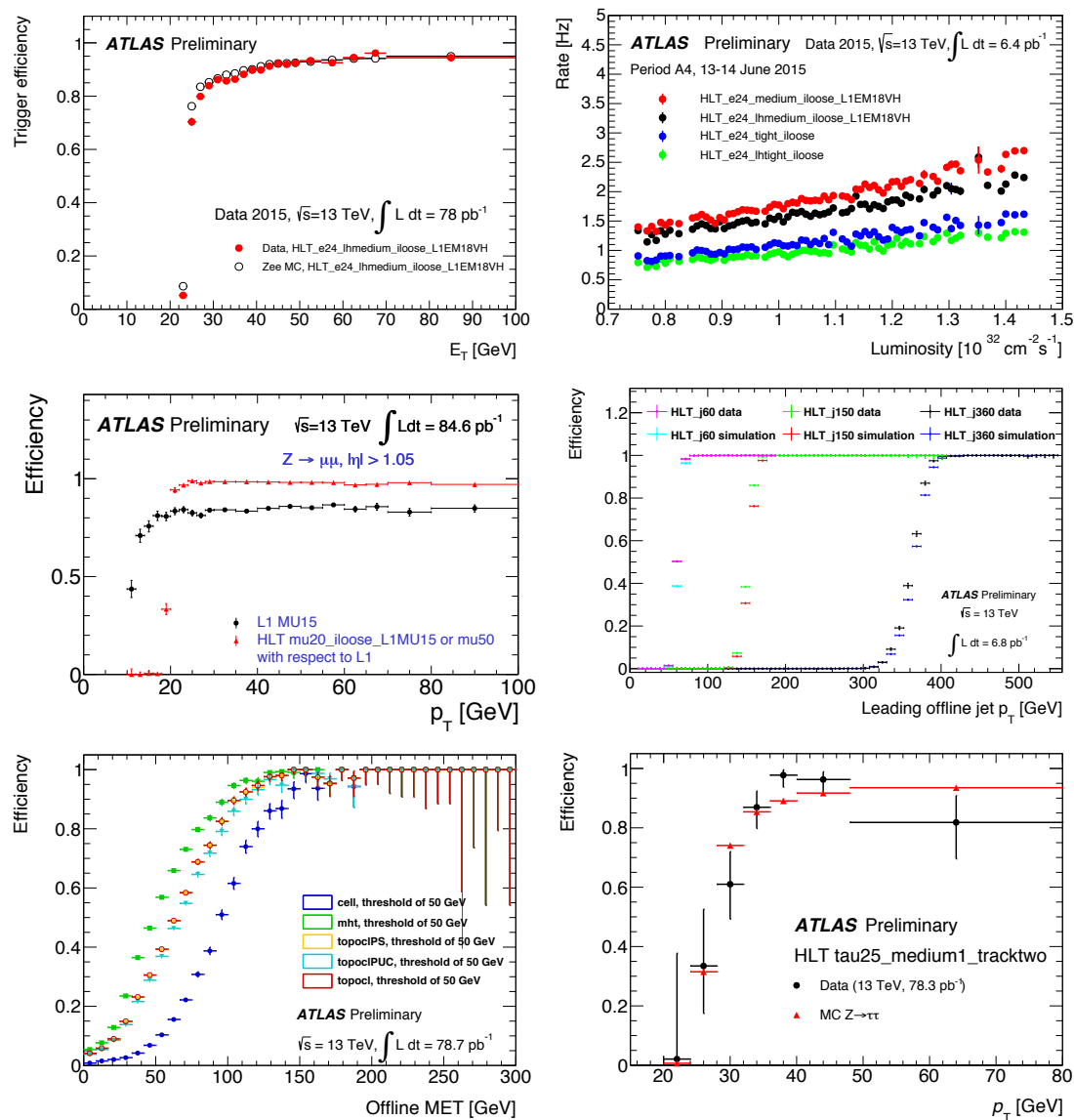


Figure 2: The performance of a selection of main physics triggers in early Run-2 is shown: The efficiency of single electron triggers and their corresponding trigger rates (top panel), the efficiency of single muon triggers (middle left), single jet triggers (middle right), missing transverse energy triggers (bottom left), and single tau lepton triggers (bottom right). Details are given in the text.

99 HLT_mu20_iloose_L1MU15 trigger is seeded by the L1_MU15 trigger and is required to satisfy a
 100 20 GeV HLT threshold and to pass a loose track isolation selection computed using inner detector
 101 tracks. The HLT_mu50 trigger is seeded by the L1_MU20 trigger and is required to satisfy a 50
 102 GeV HLT threshold. The HLT efficiency for the OR of the two HLT triggers is reported relative to
 103 the OR of the two L1 seeds. The efficiency is measured using a tag-and-probe method with $Z \rightarrow \mu\mu$
 104 candidates in 13 TeV data with 50 ns LHC bunch spacing, with no background subtraction applied.
 105 Only statistical data uncertainties are shown. More details can be found in [reference PoS LP15
 106 proceedings: “The ATLAS Muon Trigger Performance in Run I and Initial Run II Performance”

107 by Rafal Bielski].

108 Fig. 2 (middle right) shows a comparison of per-event trigger efficiency turn-on curves be-
 109 tween data and MC simulation for three typical jet trigger thresholds used during early Run-2
 110 data-taking. The HLT jets are formed from topo-clusters calibrated to the electromagnetic energy
 111 scale. The HLT jets are then calibrated to the hadronic scale by first applying a jet-by-jet area
 112 subtraction procedure followed by a jet energy scale weighting that is dependent on the HLT jet
 113 transverse momentum and pseudorapidity. Each efficiency is determined using events retained with
 114 a lower threshold trigger that is found to be fully efficient in the phase space of interest. More de-
 115 tails can be found in [reference PoS LP15 proceedings: “The ATLAS Jet Trigger at 13 TeV” by
 116 Giulio Grossi].

117 Fig. 2 (bottom left) shows missing transverse momentum trigger efficiency turn-on curves for
 118 a threshold of 50 GeV as a function of the offline reconstructed missing transverse energy for a
 119 number of different algorithms that are currently being commissioned: A 2-sided 2-sigma noise
 120 suppression cell-based algorithm (denoted cell), an algorithm based on topological calorimeter
 121 clusters (topoclusters) [4] with no further corrections (denoted topo-cl), a topocluster-based algo-
 122 rithm with hadronic calibration which subtracts average pseudorapidity-dependent pile-up energy
 123 per unit area (denoted topoclPS), a topocluster-based algorithm with hadronic calibration that re-
 124 quires at least one jet and performs a fit in which the transverse energy originating in pile-up colli-
 125 sions is constrained to zero (denoted topoclPUC), and an algorithm based on the sum of the trigger
 126 jet momenta (denoted mht). All algorithms reach the plateau efficiency at approximately 150 GeV
 127 and studies are currently in progress to determine the default choice for future data-taking. More
 128 details can be found in [reference PoS LP15 proceedings: “The ATLAS Transverse Momentum
 129 Trigger Evolution at the LHC towards Run II” by Antonia Struebig].

130 Fig. 2 (bottom right) shows the combined Level-1 and HLT tau trigger efficiency measured in
 131 data and compared to simulation, with respect to offline reconstructed tau candidates with trans-
 132 verse momentum above 20 GeV, one or three tracks and passing the offline “medium” identifica-
 133 tion criteria. The corresponding trigger tau candidate is required to have a transverse momentum
 134 of at least 25 GeV, between one and three tracks and pass the trigger “medium” identification.
 135 The trigger efficiency is measured with the first 13 TeV collisions data in an enriched sample of
 136 $Z \rightarrow \tau\tau \rightarrow \mu\tau^{\text{had}}$, where the τ -lepton decays hadronically. The efficiency is plotted as function
 137 of the transverse momentum of the offline tau candidate. Only statistical uncertainties are shown.
 138 More details can be found in [reference PoS LP15 proceedings: “The ATLAS Hadronic Tau Trigger
 139 Run I and Initial Run II Strategy and Performance” by Mark Pickering].

140 4. Conclusion

141 The ATLAS trigger system has been upgraded significantly during the LHC shutdown period
 142 to sustain the more difficult data-taking conditions in Run-2 and to select the physics processes
 143 of interest with high efficiency. At L1 these new features include upgrades to the L1 calorimeter
 144 and muon systems, the L1 central trigger processor, and a conceptually new L1 topological sub-
 145 system. At the HLT the main structural change is the merging of the previously two-level system
 146 into a single event processing farm and a major redesign of the trigger reconstruction algorithms.

147 The upgraded ATLAS trigger system is currently being commissioned and first performance results
148 of the main physics triggers in this early phase of Run-2 data-taking have been presented.

149 **References**

- 150 [1] ATLAS Collaboration *JINST* **3** (2008) S08003.
- 151 [2] L. Evans and P. Bryant, *LHC Machine*, *JINST* **3** (2008) S08001.
- 152 [3] ATLAS Collaboration, *Technical Design Report for the Phase-I Upgrade of the ATLAS TDAQ System*,
153 CERN-LHCC-2013-018, ATLAS-TDR-023 (2013).
154 <https://cds.cern.ch/record/1602235>.
- 155 [4] W. Lampl et al., *Calorimeter clustering algorithms: Description and performance*,
156 ATL-LARG-PUB-2008-002 (2008). <https://cds.cern.ch/record/1099735>.